Phase-sensitively amplified wavelength-division multiplexed optical transmission systems

Research Article | Vol. 29, No. 21 / 11 Oct 2021 / Optics Express 33086
Optics EXPRESS

Phase-sensitively amplified wavelength-division multiplexed optical transmission systems

KOVENDHAN VIJAYAN,[1,*] ZONGLONG HE,[1] BENJAMIN FOO,[2] JOCHEN SCHRÖDER,[1] MAGNUS KARLSSON,[1] AND PETER A. ANDREKSON[1]

[1] *Photonics Laboratory, Department of Microtechnology and Nanoscience, Chalmers University of Technology, SE-412 96 Gothenburg, Sweden*
[2] *Infinera Corporation, 7360 Windsor Drive, Allentown, PA 18106, USA*
[*] *vijayan@chalmers.se*

Abstract: The throughput and reach in fiber-optic communication links are limited by in-line optical amplifier noise and the Kerr nonlinearity in the optical transmission fiber. Phase-sensitive amplifiers (PSAs) are capable of amplifying signals without adding excess noise and mitigating the impairments caused by the Kerr nonlinearity. However, the effectiveness of Kerr nonlinearity mitigation depends on the dispersion pre-compensation in each span. This paper investigates dense wavelength-division multiplexed PSA-amplified links using joint processing with a less complex digital domain Volterra nonlinear equalizer at the receiver. Both numerically and with experiments, it is shown that this significantly reduces the impact of the dispersion pre-compensation in each span. Also, with simulations, a substantial improvement in transmission reach is demonstrated for PSA links.

1. Introduction

The linear physical effects in the optical fiber that distorts the signal in optical communication links are loss and dispersion, whereas the nonlinear effect is the Kerr nonlinearity. The fiber losses are due to the scattering and absorption and can be compensated using optical amplifiers. Apart from amplifying the signal, optical amplifiers also add noise due to amplified spontaneous emission (ASE), reducing signal quality. The dispersion can be compensated with optical dispersion compensation modules or in coherent systems using digital filters. The instantaneous power-dependent refractive index leads to the Kerr effect [1]. The transmission reach in fiber links are mainly limited by the distortions caused due to the Kerr effect [2–4]. The distortions caused by the Kerr effect are deterministic to some extent and can be compensated using various techniques. Depending on the domain in which the compensation is performed, one can broadly classify them as digital, optical or hybrid techniques. Some of the digital techniques are digital back-propagation (DBP) [5,6], Volterra nonlinear equalizer (VNLE) [7–10] and nonlinear Fourier transform (NFT) [11]. The optical techniques include optical phase-conjugation (OPC) [12,13] and phase-sensitive amplifiers (PSAs) [14]. Phase-conjugated twin waves (PCTWs) [15] is a hybrid technique. The digital technique can be used along optical techniques to fall under the hybrid category [16,17].

One optical technique to mitigate the transmission span nonlinearity is to use copier-phase-sensitive amplifiers (copier-PSAs) [14]. The copier is used to create an idler which is the conjugated copy of the signal. The signal and idler co-propagates in the transmission span, experiencing correlated nonlinear distortions at higher powers. After propagation, the signal and idler are coherently added in the PSA. The coherent addition of the signal and idler fields mitigates the transmission span nonlinearity as well as providing a 0-dB quantum-limited noise figure (NF) [18]. Fiber-based PSAs with NF of 1.1 dB [19] have been demonstrated. VNLE is a digital technique where inverse filtering is performed with Volterra kernels to compensate for

#426504 https://doi.org/10.1364/OE.426504
Journal © 2021 Received 30 Mar 2021; revised 22 Jul 2021; accepted 23 Aug 2021; published 28 Sep 2021

Optics EXPRESS

the linear and nonlinear effects in the optical fiber [8]. VNLE with modified kernels has been used with OPC [16] and copier-PSAs [17] to further enhance transmission span nonlinearity mitigation.

In [17], the nonlinearity mitigation in copier-PSAs was thoroughly analyzed. It was shown that there is a residual nonlinearity after mitigation in PSAs, which depends on the link and signal parameters like loss, dispersion, length of the link, dispersion pre-compensation and signal bandwidth. Also, when employing a modified VNLE, the residual nonlinearity can be reduced, and the system performance can be improved. With single-channel numerical simulations and experiments, the performance improvement in nonlinearity mitigation was studied using the VNLE with modified kernels in PSA links. In fiber links with only one wavelength channel, the major Kerr nonlinear effect is self-phase modulation (SPM). The nonlinear interaction between frequencies within the channel spectrum leads to SPM. In wavelength-division multiplexed (WDM) systems with single-polarization signals, cross-phase modulation (XPM) becomes the dominant Kerr nonlinear effect. XPM is caused by inter-channel nonlinear interactions. PSAs are capable of mitigating both SPM [14] and XPM [20]. In the case of XPM, the residual nonlinearity after coherent superposition in PSAs increases as the interacting optical signal bandwidth increases [17]. Therefore, PSAs can mitigate SPM more effectively than XPM, which was shown with two 10-GBaud 4-QAM signals placed on a 25-GHz grid [21].

Here, we study the nonlinearity mitigation using PSAs with VNLE in dense WDM systems. We use ten 10-Gbaud 4-QAM channels multiplexed on a 12.5-GHz grid for our numerical study. We show that the dispersion pre-compensation becomes less critical when using the VNLE with modified kernels in PSA links. We also study the transmission reach enhancement for PIA and PSA links with and without VNLE. Finally, the improvement in nonlinearity mitigation using VNLE in PSA links is experimentally verified using a single-span dispersion pre-compensation sweep with three 10-Gbaud 4-QAM channels separated by 12.5 GHz.

2. Phase-sensitive parametric optical amplifiers and Volterra nonlinear equalizer

Copier-PSAs can be implemented using two-mode parametric amplifiers consisting of a signal and an idler. In this work, the degenerate pump four-wave mixing (FWM) process in highly nonlinear fibers (HNLFs) based on the $\chi^{(3)}$ nonlinearity was utilized to implement the two-mode parametric amplifiers. In single-span fiber links, the transmission span is located between the copier and the PSA. The first highly nonlinear fiber, i.e., the copier, is used to create a conjugate copy of the signal called the idler at the frequency, $\omega_I = 2\omega_p - \omega_S$, where, ω_P and ω_S are the pump and signal frequencies, respectively. At the output of the copier, the generated idler, the signal and the pump are frequency- and phase-locked to achieve phase-sensitive (PS) operation in the PSA. However, the idler will not be an exact conjugate of the signal when reaching the PSA due to chromatic dispersion in the transmission span. To achieve PS operation in the second HNLF, i.e., in the PSA, the dispersion needs to be compensated, which means that copier-PSA transmission links always need to be dispersion compensated. Apart from dispersion, at high powers, the signal and idler experiences correlated Kerr nonlinear distortions. The coherent addition of the signal and idler fields in the PSA mitigates the Kerr nonlinearities [17] and also increases the signal gain by 6 dB [19] relative to operation in phase-insensitive mode. Therefore, a 6-dB noise figure improvement can be obtained considering only the signal power. In the linear regime, around 6-dB higher sensitivity [14,21,22] can be obtained for single-span links and approximately four times higher reach [23–25] for multi-span links with PSAs compared to PIAs. Moreover, the copier-PSA is modulation format independent [26] and WDM compatible [21,23].

In the weakly nonlinear regime, i.e., when the signal and the idler experience small nonlinear distortions, the electric field of signal and idler after propagation in the transmission with fully compensated loss and dispersion can be written as [17,27], $E_{\mathrm{S/I}}(\omega, L) = E_{\mathrm{S/I}}(\omega, 0) + \delta_{\mathrm{NL,S/I}}(\omega, L)$,

Optics EXPRESS

where $E(\omega)$ is the field, δ_{NL} is the nonlinear distortion approximated to the first order and L is the length of the span. For a dispersion compensated link, i.e., the accumulated dispersion is zero, without distributed Raman amplification and considering only up to second order dispersion [17,27,28],

$$\delta_{\mathrm{NL,S}}(\omega, L) = j\gamma \int_{-\infty}^{\infty}\int_{-\infty}^{\infty} \frac{1-\exp(-\alpha L + j\Delta\Omega\beta_2 L)}{\alpha - j\Delta\Omega\beta_2}\exp(-j\Delta\Omega D_0) \times E_{\mathrm{S}}(\omega_1, 0)E_{\mathrm{S}}^{*}(\omega_2, 0)E_{\mathrm{S}}(\omega-\omega_1+\omega_2, 0)d\omega_1 d\omega_2, \tag{1}$$

where, α is the fiber loss parameter, β_2 is the group velocity dispersion parameter, $\beta_2\Delta\Omega = \beta_2(\omega_1-\omega)(\omega_1-\omega_2)$ is the group velocity mismatch between the interacting frequency components, and D_0 is the dispersion pre-compensation. D_0 can take values betweeen 0 and $\beta_2 L$. PSAs are capable of partially mitigating the transmission span Kerr nonlinearity while a residual part will remain. The residual nonlinear distortions after the coherent superposition in the PSA is given by [17], $\delta^{\mathrm{res}}_{\mathrm{NL,S}}(\omega, L) = 0.5(\delta_{\mathrm{NL,S}}(\omega, L) + \delta_{\mathrm{NL,I}}(\omega, L))$. Assuming that the signal and idler are propagated in spans with identical fiber parameters, then the residual nonlinear distortions for PSA links is given by [17,29],

$$\delta^{\mathrm{res}}_{\mathrm{NL,S}}(\omega, L) = j\gamma \int_{-\infty}^{\infty}\int_{-\infty}^{\infty} j\,\mathrm{Im}\left\{\frac{1-\exp(-\alpha L + j\Delta\Omega\beta_2 L)}{\alpha - j\Delta\Omega\beta_2}\exp(-j\Delta\Omega D_0)\right\} \times E_{\mathrm{S}}(\omega_1, 0)E_{\mathrm{S}}^{*}(\omega_2, 0)E_{\mathrm{S}}(\omega-\omega_1+\omega_2, 0)d\omega_1 d\omega_2. \tag{2}$$

The effectiveness of nonlinearity mitigation in PSA links is inversely proportional to $\delta^{\mathrm{res}}_{\mathrm{NL}}(\omega, L)$, i.e., a lower value of $\delta^{\mathrm{res}}_{\mathrm{NL}}(\omega, L)$ means that the PSA mitigates the nonlinearity more effectively and vice versa. From (2), we can see that the effectiveness of nonlinearity mitigation depends on the span power map, which is dictated by α, the span dispersion map given by D_0, and the bandwidth of the optical signal. Using a single channel and different symbol rates, the optical signal bandwidth dependence on the effectiveness of nonlinearity mitigation was studied in [30]. By increasing the number of 10-Gbaud channels on a 12.5-GHz grid, the optical signal bandwidth was increased, and the effectiveness of nonlinearity mitigation for dense WDM PSA links was studied in [23]. In both scenarios, the effectiveness of nonlinearity mitigation in PSAs decreased with increasing optical signal bandwidth. The above analysis can be extended to multiple span links. Since the nonlinear distortions are small compared to the signal, the total in N spans is approximately equal to N times the distortions in each span due to the coherent addition.

The propagation of single-polarization signals with both the linear and nonlinear effects can be modelled using the scalar nonlinear Schrödinger equation (NLSE) [1]. A Volterra series transfer function (VSTF) with frequency domain kernels can be used to solve the NLSE [31]. The nonlinear perturbation coincides with the VSTF such that the N^{th} order nonlinear perturbation corresponds to the VSTF with $(2N + 1)$ kernel terms. In the optical fiber, due to inversion symmetry of fused silica, the second-order nonlinear effects are absent and therefore, the even kernels can be neglected. One way to compensate for linear and nonlinear effects is to apply the inverse VSTF to the signal after propagation, known as the Volterra nonlinear equalizer (VNLE). VNLE to compensate linear and nonlinear effects in N spans of length L with up to third-order kernels is [10],

$$E(\omega, 0) \approx K_1(\omega, NL)E(\omega, NL) + \Gamma\int_{-\infty}^{\infty}\int_{-\infty}^{\infty} F(\Delta\Omega, L, N)K_3(\Delta\Omega, L)E(\omega_1, NL)E^{*}(\omega_2, NL)E(\omega-\omega_1+\omega_2, NL)d\omega_1 d\omega_2, \tag{3}$$

where, $K_1(\omega, NL)$ is the first order linear kernel to compensate for fiber loss and dispersion, $K_3(\Delta\Omega, L)$ is the third order kernel to mitigate the nonlinear effects to the first order with

Optics EXPRESS

$F(\Delta\Omega, L, N)$ and Γ. $F(\Delta\Omega, L, N)$ takes into account the coherent addition of nonlinearities in each span as a phased-array effect and $\Gamma = -j\gamma K_1(\omega, NL)$ is the frequency dependent nonlinear term. In our case, as the transmission span is loss and dispersion compensated, i.e., the fiber attenuation and dispersion are compensated after every span, $K_1(\omega, NL) = 1$. Also, as the nonlinear distortions in each span are small compared to the signal and the coherent addition of the signal fields lead to $F(\Delta\Omega, L, N) = N$. For PIA and PSA links, the third order kernels [17] are given by

$$K_3^{PIA}(\Delta\Omega, L) = \frac{1 - \exp(-\alpha L + j\Delta\Omega\beta_2 L)}{\alpha - j\Delta\Omega\beta_2}\exp(-j\Delta\Omega D_0), \tag{4}$$

$$K_3^{PSA}(\Delta\Omega, L) = j\,\mathrm{Im}\left\{\frac{1 - \exp(-\alpha L + j\Delta\Omega\beta_2 L)}{\alpha - j\Delta\Omega\beta_2}\exp(-j\Delta\Omega D_0)\right\}, \tag{5}$$

corresponding to $\delta_{\mathrm{NL,S}}(\omega, L)$ and $\delta^{\mathrm{res}}_{\mathrm{NL,S}}(\omega, L)$, respectively. At high launch powers, the actual nonlinear distortions in PIA links are larger than the residual nonlinear distortions in PSA links. This makes the combination of VNLE with PSAs to be more effective than with PIAs.

3. Numerical investigation

3.1. Simulation model

To study the tolerance to dispersion pre-compensation in WDM PSA links when using a VNLE and to compare the performance of PIA and PSA WDM links with and without VNLE, numerical simulations were performed in MATLAB. The block diagram for PIA and PSA link simulations are shown in Fig. 1. Ten-channels of 10-Gbaud single-polarization 4-QAM signal multiplexed on a 12.5-GHz grid was used for this study. Each channel was made of 2^{16} 4-QAM symbols from random bits shaped with root-raised cosine filter of 10% roll-off and oversampled by 64 times before multiplexing them together. For all the links, the transmitter imperfections were added to the generated WDM signal in the form of additive white gaussian noise (AWGN), after which each channel's SNR was 31 dB. The WDM signal was then amplified with a booster of 4-dB NF to obtain the required launch power, P_{IN} at the input of the transmission span. The P_{IN} corresponds to the signal launch power in one channel. An 80 km standard single-mode fiber (SSMF) with the following parameters: $\alpha = 0.2$ dB/km, $D = 16$ ps/nm/km, and $\gamma = 1.3$ rad/W/km, was used as the transmission span. For propagation, the NLSE was solved numerically using the split-step Fourier method. In the case of the PSA links, an ideal conjugator was used as the copier. The signal and idler were propagated in separate split-step solvers with the same fiber parameters assuming that there is no nonlinear interactions between them. The transmission span was dispersion compensated with two dispersion compensating modules (DCMs), one before and one after the span. The DCMs were assumed to be ideal with no loss or nonlinearity. The two DCMs were used to optimize the dispersion pre-compensation. The effectiveness of nonlinearity mitigation depends on the dispersion pre-compensation for the PSA links [14] which needs to be optimized.

In the PIA link, inline phase-insensitive amplification was performed using an optical amplifier with an NF of 4 dB. The signal and idler after propagation were first amplified with optical amplifiers of 1-dB NF for the PSA link. Then, the idler was conjugated and added coherently to the signal similar to [14,23,26] to emulate the phase-sensitive amplification. For multi-span transmission systems, the blocks within the dashed box were repeated for every span. At the receiver, for both the PIA and PSA links, only the signal was detected to perform digital signal processing (DSP) and to measure the received signal quality. In the DSP, each channel was downsampled to two samples per symbol, and a constant modulus algorithm (CMA) was used for adaptive equalization. Then, the signal was downsampled to one sample per symbol to perform carrier phase estimation (CPE) using Viterbi-Viterbi. The error vector magnitude (EVM) in

Optics EXPRESS

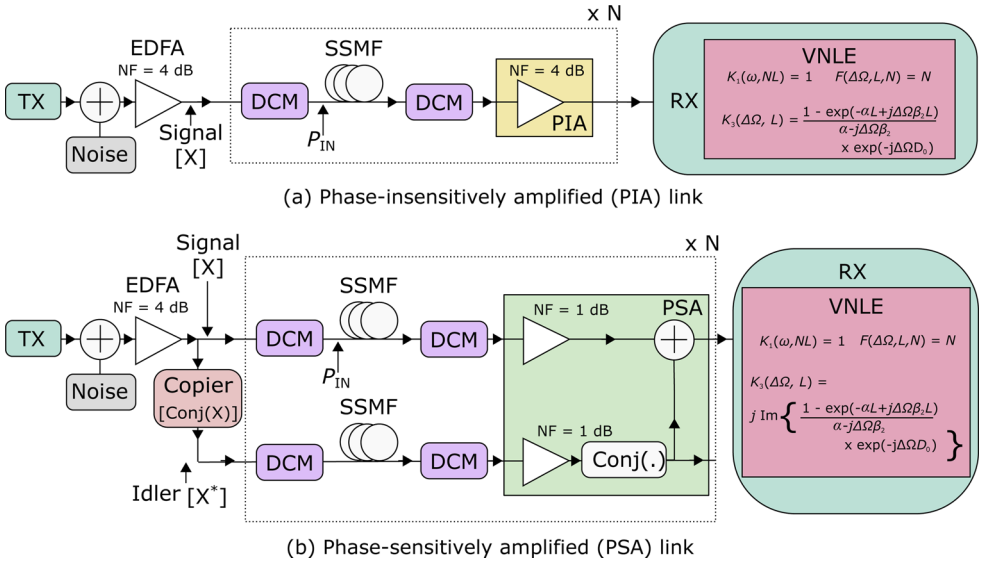

Fig. 1. Simulation model for the single- and multi-span PIA and PSA links with VNLE.

decibels (dB) for M symbols was calculated as,

$$\text{EVM (dB)} = 10\log_{10}\left(\frac{\sum_{n=1}^{M}|S_{Tx}(n)-S_{Rx}(n)|^2}{\sum_{n=1}^{M}|S_{Tx}(n)|^2}\right). \tag{6}$$

The received bits were obtained from the received symbols through de-mapping. The bit-error-rate (BER) was calculated by comparing the received and transmitted bit sequences.

For the VNLE, all ten channels were detected synchronously, and the entire signal band was downsampled to 32 samples per symbol. The VNLE with the kernels as shown in Fig. 1 for PIA and PSA links was applied on the entire WDM signal. The FFT block sizes were optimized for each links in the VNLE. Then the WDM channels were demultiplexed, and the above-mentioned DSP steps, as in the case of the separately detected single-channel, were carried out.

3.2. Simulation results

At P_{IN} = 4 dBm, dispersion pre-compensation was swept for single-span links to study the tolerance of the dispersion pre-compensation in PSA links with VNLE. Dispersion pre-compensation is the fraction of dispersion compensation applied before the fiber span relative to the total dispersion compensation required to fully compensate the transmission span dispersion. The EVM is plotted against the dispersion pre-compensation for PIA and PSA links with VNLE (right) and without VNLE (left) in Fig. 2. The shaded region indicates the spread of EVMs for the ten channels. The red shaded region corresponds to the PIA link and the grey shaded region indicates the PSA link. For the PIA link with and without VNLE, the EVM curves were flat with the difference between maximum to minimum EVMs across dispersion pre-compensation for the same channel almost being zero. However, the EVM with VNLE is better than without and the spread of the ten channels slightly decreased. The optimum dispersion pre-compensation in PSA links depends on the signal properties and for our simulated PSA-WDM signal was found to be 12.5%. Also a large difference between the maximum and minimum EVM values were seen. This shows that the dispersion pre-compensation plays an important role in the nonlinearity mitigation of PSA links and hence in its performance. With the VNLE, the EVM is improved and the curve is flat with almost no difference between the maximum and minimum EVMs for

Optics EXPRESS

all dispersion pre-compensation ratios. In PSA links, the residual nonlinearity increases with non-optimal dispersion pre-compensation and using VNLE this residual nonlinearity can be reduced. Therefore, using VNLE with PSA, the nonlinearity mitigation is improved as well as the dependence of nonlinearity mitigation on the dispersion pre-compensation can be almost eliminated.

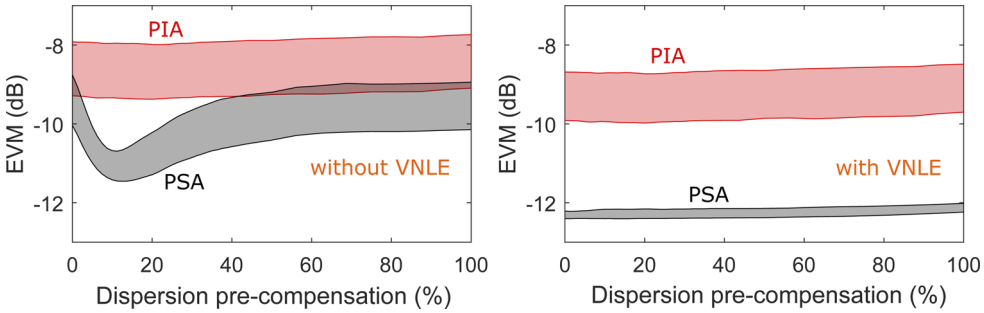

Fig. 2. Dispersion pre-compensation versus EVM for both PIA (red shaded region) and PSA (grey shaded region) links with ten-channel 10-Gbaud WDM signal. The left figure is without VNLE and the right figure includes VNLE.

The launch power, P_{IN}, was swept to compare the performance of PIA and PSA links with and without VNLE. The transmission reach was calculated at BER = $1\text{x}10^{-3}$ with optimum dispersion pre-compensation and plotted versus launch power for both PIA and PSA links in Fig. 3. On the left is without VNLE and the right figure corresponds to with VNLE. The transmission reach is four times higher in the linear regime ($P_{\mathrm{IN}} = -20$ dBm) as expected for PSA links compared to PIA links with and without VNLE due to low-noise amplification. Considering the worst-performing channel, the optimum launch powers for PIA and PSA links are -13 and -14 dBm respectively without VNLE. At optimum launch powers, the reach is 3.2 times higher for PSA links with respect to PIA links. The reach improvement is from both low-noise amplification and nonlinearity mitigation. With VNLE, the optimum launch power of the PSA link increases by 2 dB to -12 dBm. The reach improvement comparing PSA and PIA links with VNLE was 4.6 times. The VNLE improves the transmission reach for the PSA links by approximately 1.5 times, whereas a very small improvement is obtained for the PIA links. The residual nonlinear distortions after the PSAs are small compared to the actual nonlinear distortions in the PIA links in each span. For multi-span links, these distortions are coherently added as the links are dispersion compensated. The modified VNLE is applied for both PIA and PSA links in one step

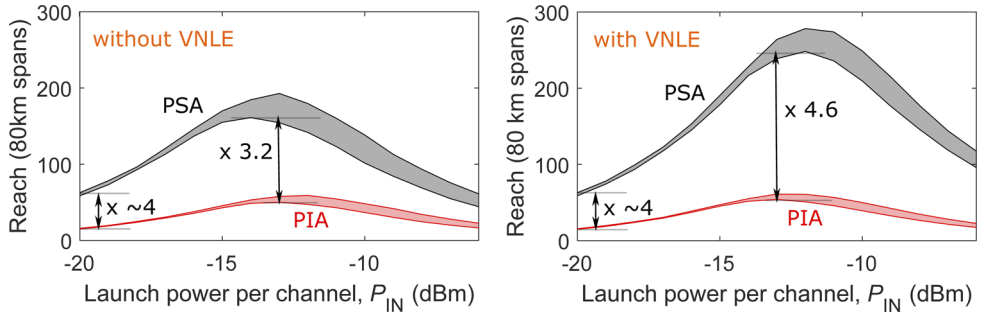

Fig. 3. Launch power versus transmission reach for both PIA (red shaded region) and PSA (grey shaded region) links with ten-channel 10-Gbaud WDM signal. The left figure is without VNLE and the right figure includes VNLE.

Optics EXPRESS

after total transmission. We believe that the combination of PSAs with VNLE is more effective compared to PIAs with VNLE due to the smaller residual nonlinear distortions in PSA links.

4. Experiments

4.1. Experimental setup

We performed proof-of-concept experiment to verify the enhancement of nonlinearity mitigation in WDM PSA links with VNLE with the setup shown in Fig. 4. Three external cavity lasers (ECLs) operating at 1550.0 nm, 1550.1 nm, and 1550.2 nm were modulated individually with 10-Gbaud amplified electrical signals. The RF signal for each channel consisted of 2^{16} random symbols corresponding to 4-QAM modulation format shaped with root-raised cosine filter of 10% roll-off. All the three channels were then combined together to obtain the transmitted signal as shown in the inset. The transmitted signal was combined with a high power pump at 1554.1 nm and fed to the first 150 m strained HNLF, which acted as the copier. The copier produced the conjugated copy of the signal called the WDM idler centered at 1558.1 nm. Another inset in Fig. 4 shows the generated idler. The pump power into the copier HNLF was set around 28 dBm, limited by the stimulated Brillouin scattering (SBS). The signal and idler were separated from the high power pump. The high power pump was attenuated with a variable optical attenuator (VOA) to produce a weak pump tone to avoid nonlinear effects in the transmission span. In the power-balancing stage, the WDM signal and idler were balanced, and the required signal launch power per channel P_{IN} was set using an EDFA, a waveshaper (WS) and a variable optical attenuator (VOA). The attenuated weak pump was combined with the balanced signal and idler and launched into the compensated link. The dispersion-compensated link consisted of an 80 km standard single-mode fiber (SSMF), with two channelized tunable fiber-Bragg gratings (FBGs) based DCMs. The transmission fiber was inserted between the two FBG based DCMs to sweep the dispersion pre-compensation. The dispersion in the transmission span was 1275 ps/nm. After the dispersion-compensated link, the signal and idler were again separated from the weak pump tone. Optical injection locking was used in the pump recovery to obtain a high power, phase- and frequency-locked pump wave from the weak pump tone for the PSA at the receiver. The signal and idler were separated to align them in time and polarization in the re-timing and polarization tuning stage. A variable delay line was used for time synchronization. A VOA was also used to balance the WDM signal and idler for wavelength-dependent loss in the dispersion-compensated link. The WDM signal and idler were combined with the high power pump wave after another VOA used to set the required power at PSA input. The PIA/PSA contains four spools of strained HNLFs with isolators in between them to increase the SBS threshold, measuring approximately 600 m. For the strained HNLF, the average zero-dispersion wavelength was 1544 nm, and at 1550 nm, the average dispersion parameter (D), the dispersion slope (S) and the nonlinear coefficient (γ) were 0.45 ps/nm/km, 0.072 ps/nm^2/km and 9.7 rad/W/km respectively. The pump power into the PIA/PSA was set to be around 30 dBm, limited by SBS. A phase-locked loop was used to compensate for the phase fluctuations and stabilize the phase-locking between the signal, idler and pump waves to maintain maximum PSA gain. In the case of the PIA, the high power pump after the copier was completely attenuated, and the idler was blocked in the WS. Only the signal was transmitted. The PIA gain was 16 dB, whereas the PSA gain was 22 dB. The PSA had a 6 dB additional gain due to coherent superposition of the signal and idler [19]. After the PIA/PSA, the three channels occupying a bandwidth of 35 GHz were detected together with a coherent receiver and a real-time scope of analog bandwidth 22 GHz and 33 GHz, respectively. Then, the captured signal was processed as shown in the DSP block (Fig. 4). The DSP blocks were implemented using QAMPy [32] apart from the VNLE. The signal was scaled to the corresponding launch power, P_{IN} before applying the VNLE in the digital domain.

Optics EXPRESS

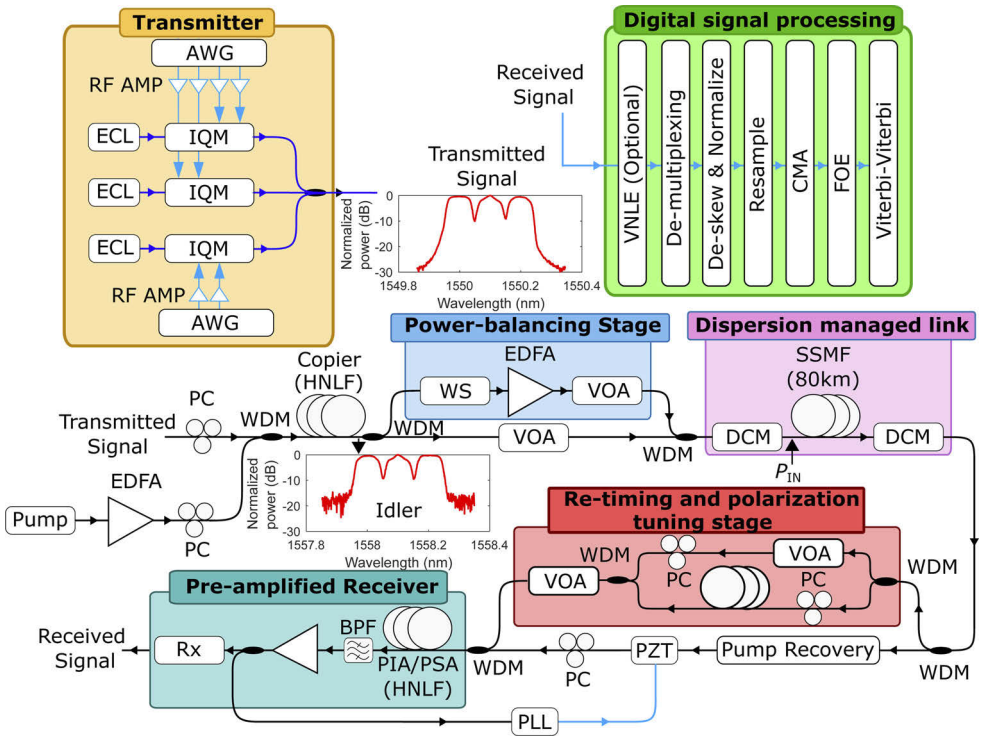

Fig. 4. Experimental setup used for single-span WDM fiber transmission with phase-(in)sensitive amplifiers as pre-amplifiers: ECL - External-cavity laser, AWG - Arbitrary waveform generator, RF AMP - Radio-frequency amplifier, IQM - IQ modulator, PC - Polarization controller, EDFA - Erbuim-doped fiber amplifier, WDM - Wavelength-division-multiplexing coupler, WS - WaveShaper, DCM - Dispersion compensation module, VOA - Variable optical attenuator, SSMF - Standard single-mode fiber, PZT - Piezoelectric transducer, PIA - Phase-insensitive amplifier, PSA - Phase-sensitive amplifier, BPF - Optical bandpass filter, Rx - Coherent receiver. Inset- Spectra of transmitted signal and idler after copier.

4.2. *Experimental results*

To verify the performance improvement when using VNLE in WDM PSA links, a dispersion pre-compensation sweep was performed using the three-channel 10-Gbaud 4-QAM WDM signal for both PIA and PSA links, with and without VNLE. The launch power per channel, P_{IN} was set to 8 dBm. The EVM and BER were measured and plotted versus the dispersion pre-compensation for both PIA and PSA links in Fig. 5. The top-left figure contains the EVM plots without VNLE, whereas the top-right shows the EVM plots with VNLE. The BER plots without and with VNLE are in the bottom-left and bottom-right, respectively. The blue, red and black curves correspond to channel 1, 2 and 3, respectively, where channel 2 is the center channel. The channel 2 experiences stronger XPM from both the other channels and therefore has the worst performance of all the channels. PIA links are represented by dotted lines with circle markers, and the solid lines with diamond markers correspond to PSA links. The BER and EVM curves exhibit a similar trend. The dispersion pre-compensation sweep for the PIA link without VNLE gave a flat response, indicating that the dispersion pre-compensation does not significantly affect the PIA links. For the PSA without VNLE, the optimum dispersion pre-compensation was slightly different for the three channels. The average optimum dispersion pre-compensation from EVMs for the three channels

Optics EXPRESS

corresponds to 14.7%. It was not possible to obtain the optimum dispersion pre-compensation values from the BERs due to the error floor. The dispersion pre-compensation dependence on the link performance was significant for the PSA links. With VNLE, the signal performance improved, and the curves became much flatter as the difference between the maximum and minimum values decreased for the PSA links. However, the optimum values remained the same for the EVMs. The PIA links with VNLE performed worse than without VNLE, which we believe is due to the dispersion pre-compensation sweep performed at substantially higher launch powers. However, this needs further investigation. The experimental demonstration verifies that the VNLE enhances nonlinearity mitigation in PSA links and reduce PSA's sensitivity to the dispersion pre-compensation.

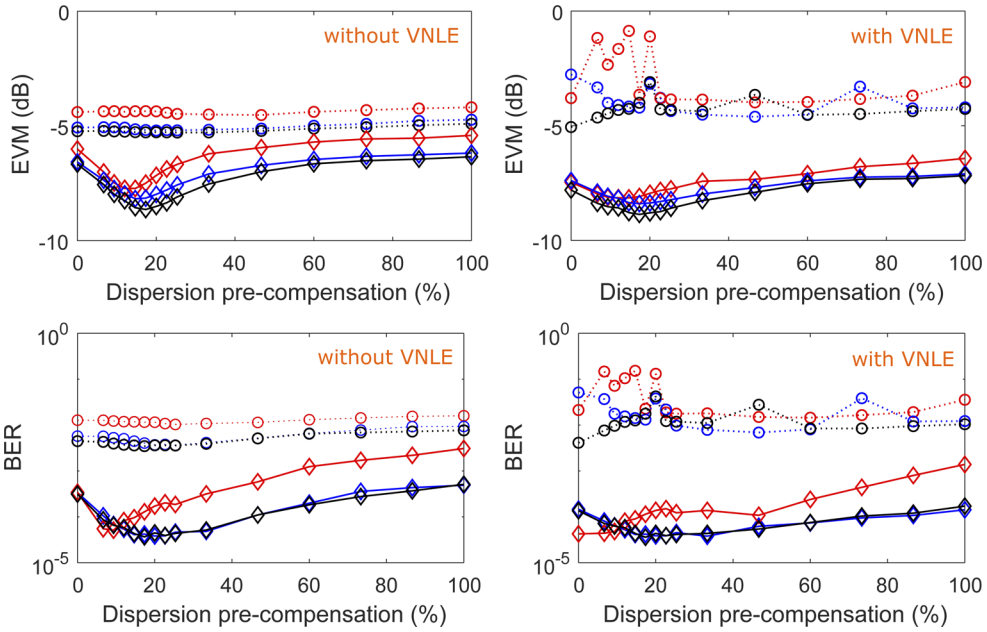

Fig. 5. Measured EVM and BER versus dispersion pre-compensation, for single-span links at P_{IN} = 8 dBm. The blue, red and black colour correspond to Channel 1, 2 and 3, respectively. The dotted lines with circle markers represent the PIA link and the solid lines with diamond markers correspond to the PSA link.

5. Discussions

The copier-PSA is capable of mitigating transmission span nonlinearity. However, there are some residual nonlinearities after mitigation in PSAs. This residual nonlinearity depends on the link and the signal. It has been shown that the residual nonlinearity increases with an increase in the number of WDM signal channels [23]. This paper shows that residual nonlinearity can be decreased by using a digital nonlinear filter in WDM PSA links. For this purpose, VNLE was used with modified kernels, as discussed in [17] and section 2. The VNLE contained kernels up to the third order and can compensate nonlinearity up to the first-order perturbation expansion in γ. Therefore, the VNLE works well only in the weakly nonlinear regime. In the simulations, first dispersion pre-compensation sweep was performed (Fig. 2) at launch power of 4 dBm and then with optimum dispersion pre-compensation, the transmission reach was obtained for different launch powers (Fig. 3). Around 1-dB EVM improvement was obtained in the pre-compensation sweep for PIA links with VNLE compared to without VNLE. However, negligible improvement

Optics EXPRESS

was obtained in terms of transmission reach for PIA links when VNLE was applied. The VNLE was applied in one step after transmission. For the dispersion pre-compensation sweep, the signals were transmitted only for one span compared to multiple spans in the launch power sweep. Therefore, the accumulated nonlinearity is higher in multi-span transmission, and this reduces the effectiveness of the VNLE. Since the PSA already removes a large part of nonlinearity due to coherent superposition of the signal and idler in each span, the modified VNLE is more effective together with PSAs compared to PIAs in multi-span transmission.

Ten channels of 10-Gbaud 4-QAM single-polarization signals closely placed on a 12.5 GHz grid were used in the numerical study to show the benefit of the modified VNLE in PSA-WDM links. However, in the proof-of-concept experiment, only three channels were used due to bandwidth limitations arising from the channelized tunable FBG-based DCMs and the gain bandwidth of the fiber-optic parametric amplifier (PIA/PSA). Moreover, the PSA links with VNLE in simulations perform better than in the experiments and also penalties were seen for PIA links when VNLE was applied in the experiments. We attribute this to the pre-dispersion sweep conducted at higher than optimum launch power leading to more substantial nonlinear distortions in the experiments as well as many experimental imperfections. We also believe that the dispersion of HNLF used as the PIA/PSA does not affect this study as we were operating near the zero-dispersion wavelength as well the signal bandwidth was small.

In this work, all the WDM channels were jointly detected and processed with VNLE. However, the VNLE can also be applied on the individual channel, which does not require them to be detected jointly. This would reduce the complexity of the detection setup, especially with many WDM channels. However, applying VNLE channel-wise had negligible reach improvement compared to not using VNLE, which we verified with simulations. At least in dense WDM systems, the channels are more affected by cross-phase modulation (XPM) than self-phase modulation (SPM). Therefore, applying VNLE channel-wise can compensate only for SPM and not for XPM, which resulted in negligible improvement.

6. Conclusion

We have shown that using VNLE with appropriately modified kernels, the residual nonlinearity in copier-PSA links can be reduced for dense WDM signals. Incorporating the VNLE in the digital domain at the receiver, the copier-PSA link's performance becomes less sensitive to transmission span dispersion pre-compensation. This has been verified both in simulations and experiments. Using numerical simulation, we also show that the transmission reach and optimum launch power increases for PSA links with VNLE.

Funding. Vetenskapsrådet (2015-00535).

Acknowledgments. We thank OFS Denmark for providing the HNLFs used for the PSA. The simulations were performed on resources at Chalmers Centre for Computational Science and Engineering (C3SE) provided by the Swedish National Infrastructure for Computing (SNIC).

Disclosures. The authors declare that there are no conflicts of interest related to this article.

Data availability. Data underlying the results presented in this paper are not publicly available at this time but may be obtained from the authors upon reasonable request.

References

1. G. P. Agrawal, *Nonlinear fiber optics* (Elsevier / Academic Press, 2013).
2. A. D. Ellis, J. Zhao, and D. Cotter, "Approaching the non-linear Shannon limit," J. Lightwave Technol. **28**(4), 423–433 (2010).
3. A. D. Ellis, M. E. McCarthy, M. A. Z. A. Khateeb, M. Sorokina, and N. J. Doran, "Performance limits in optical communications due to fiber nonlinearity," Adv. Opt. Photonics **9**(3), 429–503 (2017).
4. E. Agrell, A. Alvarado, G. Durisi, and M. Karlsson, "Capacity of a nonlinear optical channel with finite memory," J. Lightwave Technol. **32**(16), 2862–2876 (2014).
5. E. Ip and J. M. Kahn, "Compensation of dispersion and nonlinear impairments using digital backpropagation," J. Lightwave Technol. **26**(20), 3416–3425 (2008).

Optics EXPRESS

6. D. Rafique, M. Mussolin, M. Forzati, J. Mårtensson, M. N. Chugtai, and A. D. Ellis, "Compensation of intra-channel nonlinear fibre impairments using simplified digital back-propagation algorithm," Opt. Express **19**(10), 9453–9460 (2011).
7. F. P. Guiomar, J. D. Reis, A. L. Teixeira, and A. N. Pinto, "Digital postcompensation using volterra series transfer function," IEEE Photonics Technol. Lett. **23**(19), 1412–1414 (2011).
8. F. P. Guiomar, J. D. Reis, A. L. Teixeira, and A. N. Pinto, "Mitigation of intra-channel nonlinearities using a frequency-domain volterra series equalizer," Opt. Express **20**(2), 1360–1369 (2012).
9. L. Liu, L. Li, Y. Huang, K. Cui, Q. Xiong, F. N. Hauske, C. Xie, and Y. Cai, "Intrachannel nonlinearity compensation by inverse volterra series transfer function," J. Lightwave Technol. **30**(3), 310–316 (2012).
10. F. P. Guiomar and A. N. Pinto, "Simplified volterra series nonlinear equalizer for polarization-multiplexed coherent optical systems," J. Lightwave Technol. **31**(23), 3879–3891 (2013).
11. S. K. Turitsyn, J. E. Prilepsky, S. T. Le, S. Wahls, L. L. Frumin, M. Kamalian, and S. A. Derevyanko, "Nonlinear Fourier transform for optical data processing and transmission: advances and perspectives," Optica **4**(3), 307–322 (2017).
12. R. A. Fisher, B. R. Suydam, and D. Yevick, "Optical phase conjugation for time-domain undoing of dispersive self-phase-modulation effects," Opt. Lett. **8**(12), 611–613 (1983).
13. W. Pieper, C. Kurtzke, R. Schnabel, D. Breuer, R. Ludwig, K. Petermann, and H. G. Weber, "Nonlinearity-insensitive standard-fibre transmission based on optical-phase conjugation in a semiconductor-laser amplifier," Electron. Lett. **30**(9), 724–726 (1994).
14. S. L. I. Olsson, B. Corcoran, C. Lundström, T. A. Eriksson, M. Karlsson, and P. A. Andrekson, "Phase-sensitive amplified transmission links for improved sensitivity and nonlinearity tolerance," J. Lightwave Technol. **33**(3), 710–721 (2015).
15. X. Liu, A. Chraplyvy, P. Winzer, R. Tkach, and S. Chandrasekhar, "Phase-conjugated twin waves for communication beyond the Kerr nonlinearity limit," Nat. Photonics **7**(7), 560–568 (2013).
16. G. Saavedra, G. Liga, and P. Bayvel, "Volterra-assisted optical phase conjugation: A hybrid optical-digital scheme for fiber nonlinearity compensation," J. Lightwave Technol. **37**(10), 2467–2479 (2019).
17. B. Foo, M. Karlsson, K. Vijayan, M. Mazur, and P. A. Andrekson, "Analysis of nonlinearity mitigation using phase-sensitive optical parametric amplifiers," Opt. Express **27**(22), 31926–31941 (2019).
18. C. M. Caves, "Quantum limits on noise in linear amplifiers," Phys. Rev. D **26**(8), 1817–1839 (1982).
19. Z. Tong, C. Lundström, P. Andrekson, C. McKinstrie, M. Karlsson, D. Blessing, E. Tipsuwannakul, B. Puttnam, H. Toda, and L. Grüner-Nielsen, "Towards ultrasensitive optical links enabled by low-noise phase-sensitive amplifiers," Nat. Photonics **5**(7), 430–436 (2011).
20. K. Vijayan, B. Foo, H. Eliasson, and P. A. Andrekson, Cross-phase modulation mitigation in WDM transmission systems using phase-sensitive amplifiers, European Conference on Optical Communication (ECOC) (2018), pp. 1–3.
21. K. Vijayan, B. Foo, M. Karlsson, and P. A. Andrekson, "Cross-phase modulation mitigation in phase-sensitive amplifier links," IEEE Photonics Technol. Lett. **31**(21), 1733–1736 (2019).
22. B. Corcoran, S. L. I. Olsson, C. Lundström, M. Karlsson, and P. Andrekson, "Phase-sensitive optical pre-amplifier implemented in an 80km DQPSK link," in *OFC/NFOEC*, (2012), pp. 1–3.
23. K. Vijayan, B. Foo, M. Karlsson, and P. A. Andrekson, "Long-haul transmission of WDM signals in with in-line phase-sensitive amplifiers," in *2019 European Conference on Optical Communication (ECOC)* (2019), pp. 1–3.
24. S. L. Olsson, H. Eliasson, E. Astra, M. Karlsson, and P. A. Andrekson, "Long-haul optical transmission link using low-noise phase-sensitive amplifiers," Nat. Commun. **9**(1), 3064–3067 (2018).
25. S. L. I. Olsson, M. Karlsson, and P. A. Andrekson, "Long-haul optical transmission of 16-QAM signal with in-line phase-sensitive amplifiers," in *2017 European Conference on Optical Communication (ECOC)* (2017), pp. 1–3.
26. K. Vijayan, Z. He, B. Foo, M. Karlsson, and P. A. Andrekson, "Modulation format dependence on transmission reach in phase-sensitively amplified fiber links," Opt. Express **28**(23), 34623–34638 (2020).
27. H. Louchet, A. Hodzic, K. Petermann, A. Robinson, and R. Epworth, "Simple criterion for the characterization of nonlinear impairments in dispersion-managed optical transmission systems," IEEE Photonics Technol. Lett. **17**(10), 2089–2091 (2005).
28. J. K. Fischer, C. Bunge, and K. Petermann, "Equivalent single-span model for dispersion-managed fiber-optic transmission systems," J. Lightwave Technol. **27**(16), 3425–3432 (2009).
29. X. Liu, S. Chandrasekhar, P. J. Winzer, R. W. Tkach, and A. R. Chraplyvy, "Fiber-nonlinearity-tolerant superchannel transmission via nonlinear noise squeezing and generalized phase-conjugated twin waves," J. Lightwave Technol. **32**(4), 766–775 (2014).
30. K. Vijayan, H. Eliasson, B. Foo, S. L. Olsson, M. Karlsson, and P. A. Andrekson, "Optical bandwidth dependency of nonlinearity mitigation in phase-sensitive amplifier links," in *2018 European Conference on Optical Communication (ECOC)*, (IEEE, 2018), pp. 1–3.
31. K. V. Peddanarappagari and M. Brandt-Pearce, "Volterra series transfer function of single-mode fibers," J. Lightwave Technol. **15**(12), 2232–2241 (1997).
32. J. Schröder and M. Mazur, "QAMPy a DSP chain for optical communications, DOI: 10.5281/zenodo.1195720,".